(Procs. Conference on High Angular Momentum Properties of Nuclei, Oak Ridge, Tennessee, November 2-4, 1982, Harwood, NY)

CONF-821143--5

CONF-821143--5

DE83 008190

HIGH SPINS IN GAMMA-SOFT NUCLEI

G. A. LEANDER
UNISOR, Oak Ridge Associated Universities
Oak Ridge, TN 37830, U.S.A.

S. FRAUENDORF*
University of Tennessee
Knoxville, TN 37916, U.S.A.

AS05-76ER04936

F. R. MAY
Central Institute for Nuclear Research
Rossendorf, G.D.R.

Abstract Nuclei which are soft with respect to the γ shape degree of freedom are expected to have many different structures coexisting in the near-yrast regime. In particular, the lowest rotational quasi-particle in a high-j shell exerts a strong polarizing effect on γ. The γ to which it drives is found to vary smoothly over a 180° range as the position of the Fermi level varies. This simple rule is seen to have a direct connection with the energy staggering of alternate spin states in rotational bands. A diagram is presented which provides a general theoretical reference for experimental tests of the relation between γ, spin staggering, configuration, and nucleon number. In a quasicontinuum spectrum, the coexistence of different structures are expected to make several unrelated features appear within any one slice of sum energy and multiplicity. However, it is also seen that the in-band moment of inertia may be similar for many bands of different γ.

*Permanent address: Central Institute for Nuclear Research, Rossendorf, G.D.R.

I. INTRODUCTION

Nuclear structure calculations indicate that the intrinsic shape of some nuclei is soft with respect to γ, the angular coordinate which measures triaxiality in a polar representation of quadrupole shapes (e.g. Refs. 1-7). Many more nuclei are expected to become γ-soft in some range of high spins where the structure and shape undergo change[8,9]. It is known that such flatness of the adiabatic potential-energy surface in the γ-direction is a necessary though insufficient condition for low-energy collective γ-vibrations. This paper, however, is concerned with another aspect of γ-softness, namely that the average 'static' shape can be strongly influenced by small changes of the configuration. Significant variations of γ between different configurations, due to the γ-softness, can lead to the coexistence of states or families of states in the yrast region with very different spectroscopic character. At some γ-values rotation is largely collective and generates bands or regularly spaced levels connected by enhanced E2 transitions, while at other γ-values the rotation takes place around a symmetry axis and gives rise to an irregular spectrum of aligned single-particle states.

Our convention[8] for the axis of rotation relative to the shape as a function of γ is illustrated in Fig. 1. The single-particle limit is reached at $+60°$ and $-120°$, while maximum collectivity occurs at $-30°$. A semiclassical axis of rotation can be defined since rotation is treated in this paper in the framework of cranking. A technical description of the methods employed can be found in the literature (Refs. 10 and 11 and other references below).

The present study of rotations in γ-soft nuclei proceeds stepwise, treating subsystems that might be viewed as

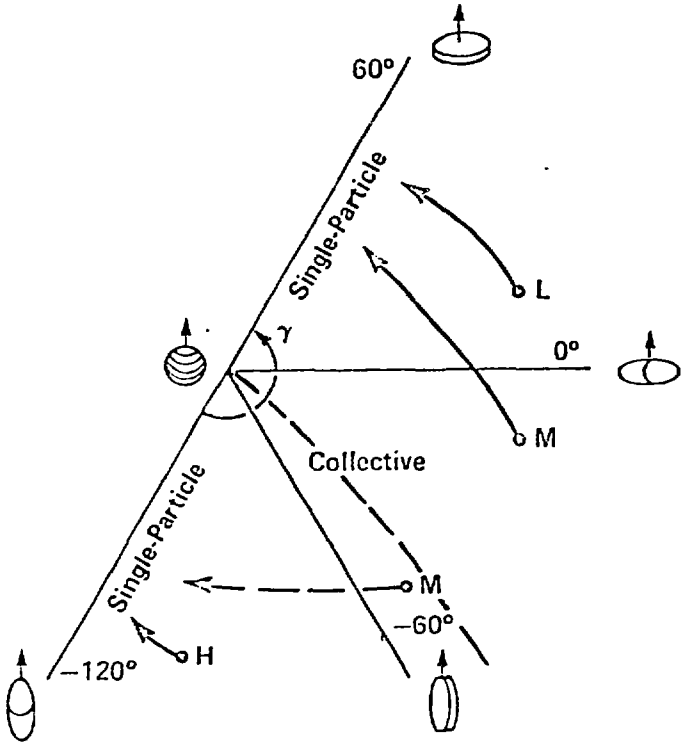

FIGURE 1. Quadrupole shapes in a polar coordinate plane. The radius, ε, measures the deviation from spherical shape. The angle, γ, gives the triaxiality and the orientation with respect to the axis of rotation. Arrows indicate shape changes with increasing spin in the L-, M-, and H-bands of Section III below.

the basic constituents of nuclear rotation. Section II considers rotation in a single j-shell, the resulting γ-polarization effects and ways to identify these effects in experimental discrete-line spectra. Section III describes rotations in a harmonic oscillator potential. Adding these components together, one obtains, loosely speaking, the more realistic model of a rotating modified oscillator[8,12]. Results of the modified oscillator model are discussed in Section IV. A question of particular interest is whether

coherent structural features can be expected to emerge in the high-spin quasicontinuum spectra of γ-soft nuclei.

II. HIGH-J QUASI-PARTICLE EFFECTS

The first step is to study the orbitals of a high-j shell at finite rotational frequency as a function of γ. For this purpose, the rotating quasi-particle states in the N=5 shell of a cranked modified oscillator potential have been calculated with pairing included. The value of γ is varied smoothly from $-120°$ to $+60°$ at a fixed distance ($\varepsilon = 0.2$) from the origin in the quadrupole deformation plane. The results are not sensitive to the precise choice of distance from the origin within the range of values that is characteristic for γ-soft nuclei at moderately high spins. The Fermi level parameter λ is also varied through a sequence of values corresponding to different positions in the $h_{11/2}$ shell. The latter is the high-j shell which comes at the bottom of the modified oscillator N=5 shell due to the spin-orbit interaction. The general results below are probably not specific to $h_{11/2}$, and can be viewed as representative for any high-j shell. The pairing gap parameter Δ is held fixed at the value 0.1 $\hbar\omega_o$ in the calculation and the rotational frequency ω is held fixed at 0.03 $\hbar\omega_o$, which is near and in most cases just below the first backbend. The quantity extracted from the cranking solutions is not the total energy of the nucleus in this case, but the energy e^{ω} of the lowest $h_{11/2}$ diabatic quasi-particle states as a function of γ. In regions of γ where a band crossing happens to occur precisely at the fixed rotational frequency ω of the present calculation, the diabatic levels are obtained graphically by extending the adiabatic levels from other regions of γ straight through the crossing

region (c.f. Ref. 13).

The most salient feature of the results is shown in Fig. 2. Several curves are included in this plot for different positions of the Fermi level in the j-shell. The correspondence between the code numbers 1-9 on the curves in Fig. 2 and the position of the Fermi level λ is shown in

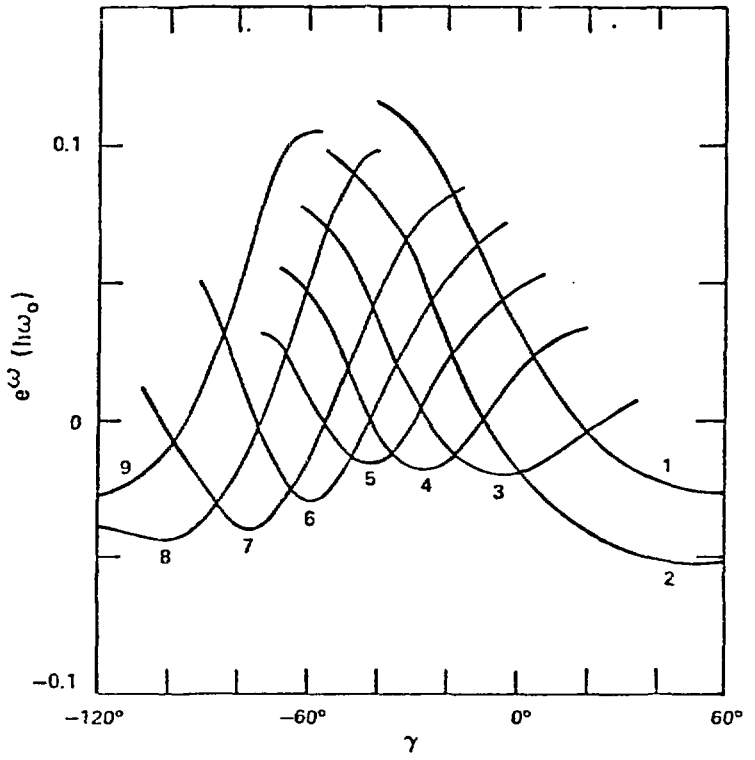

FIGURE 2. The $h_{11/2}$ favored quasi-particle routhian, plotted as a function of γ at fixed rotational frequency $\omega = 0.03\ \omega_o$ for nine different positions of the Fermi level (see Fig. 3).

Fig. 3. At number 1, λ lies below the shell and then it is raised successively until it comes above the $h_{11/2}$ shell at number 9. The curve for each λ shows e^{ω} of the lowest rotating quasi-particle state whose eigenvalue with respect

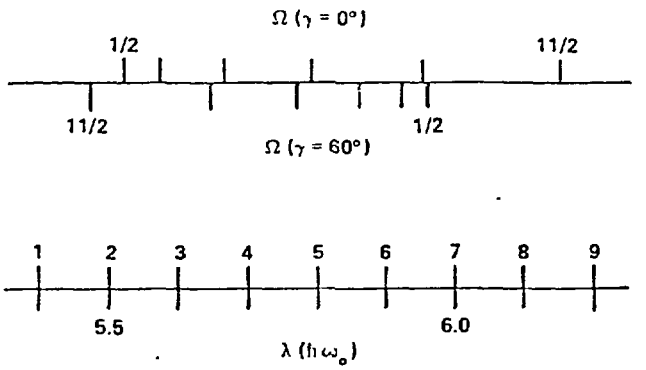

FIGURE 3. Key to the Fermi level code numbers 1-9 in Figs. 2 and 4. The lower axis shows the corresponding energies in oscillator units. The upper axis, representing the same energy range, shows the non-rotating $h_{11/2}$ single-particle levels at two γ-values, 0° and 60°.

to the symmetry operator $e^{-i\pi j_x}$ is $e^{-i\pi\alpha}$ with $\alpha = -1/2$, the so-called favored signature (α = j modulo 2) in the $h_{11/2}$ shell. The equilibrium shape is seen to be oblate for a particle state (1), and for a hole state (9) it is prolate at -120°. These are well-known results. At intermediate positions of the Fermi level λ, Fig. 2 shows a simple and logical pattern which was not known before. For each λ there is a sharp pronounced minimum at a specific value of γ, and the position of this minimum moves smoothly over the full range of γ as the Fermi level moves through the shell. There is a slight aberration from this pattern in the 0° to +60° sector, where the minimum remains at 60° until the curve becomes very flat with increasing λ and the minimum is finally tilted over towards 0°.

Consequently, the presence of a high-j quasi-particle with the favored signature in a γ-soft nucleus is expected to stabilize the shape at a γ-value which is sharply determined by the position of the Fermi level in the shell. If

the nucleus is not γ-soft, but has a potential-energy minimum at some other value of γ, the quasi-particle exerts a driving force in γ proportional to the gradient of the relevant curve in Fig. 2. Thereby, it acts to shift the γ-deformation to a point where the driving force is balanced by the restoring force of the potential.

The quasi-particle states of the unfavored signature, $\alpha = +1/2$ in the $h_{11/2}$ shell, do not exhibit such pronounced or systematic dependences on γ and λ. For λ inside the lower part of the shell, at positions 2-4 in Fig. 3, the lowest unfavored quasi-particle state has some driving effect towards positive γ, and for λ inside the upper part of the shell (6-7) there is a driving force toward large negative γ. In general, however, the unfavored orbitals have a weaker γ-dependence than the favored ones. Consequently, at the γ-value where the favored orbital goes down to its minimum, it becomes significantly lower than the unfavored orbital at any point. This effect can be seen in Fig. 4, where the solid curves are the same as in Fig. 2 but now placed in a separate subdiagram for each position 1-9 of the Fermi level λ. The dashed lines show the orbitals of the unfavored signature. These are seen to lie at the overall level of the higher-lying sections on the solid curves, well above the solid-curve minima. The seeming exceptions at positive γ in squares 8 and 9 actually confirm the rule, since the dashed curve there is the favored signature of the $h_{9/2}$ shell and repeats the pattern of squares 1 and 2.

This rule for the signature splitting, large at the preferred γ and small or even inverted at other values of γ, is a generalization of the rules known previously from the work of Stephens[14], Meyer-ter-Vehn[15], and more

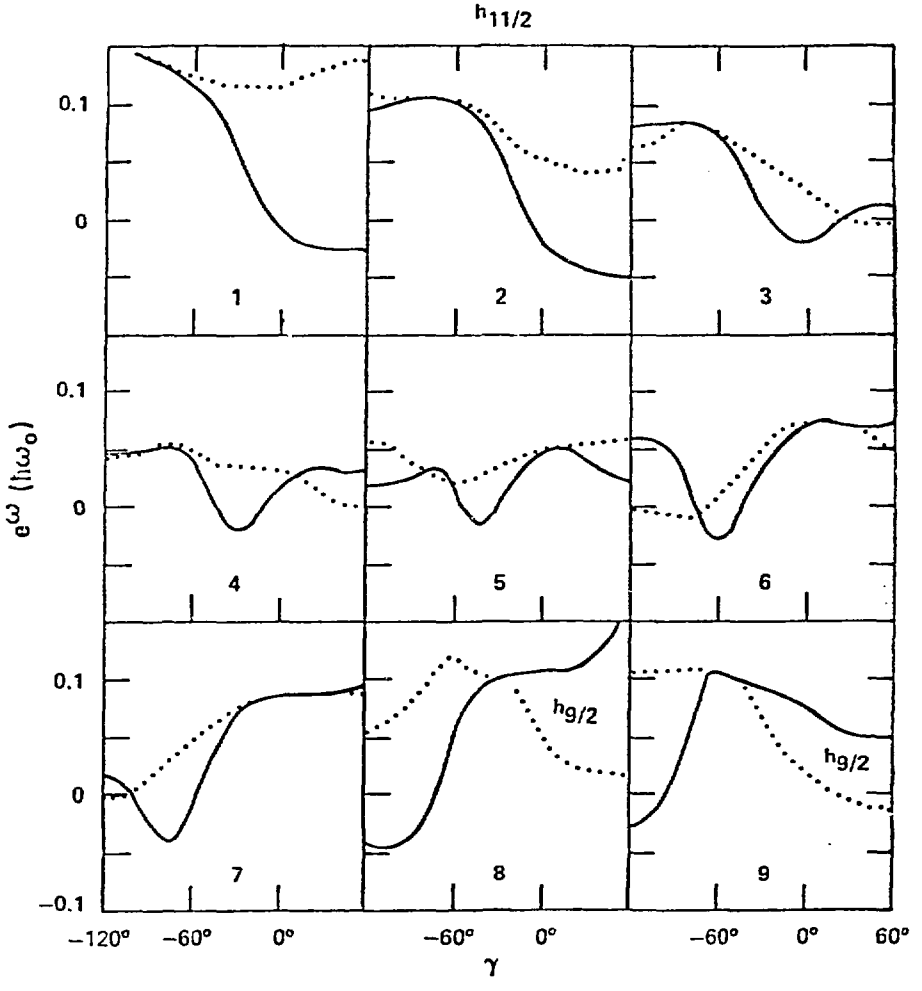

FIGURE 4. The interplay between γ and rotational quasi-particles. The solid curves show favored $h_{11/2}$ diabatic routhians, the same as in Fig. 2. The dashed curves show the lowest routhian of the other signature. The splitting between the dashed and solid lines is the one-quasi-particle signature splitting which is observable in experiment. Note the large signature splitting at the minimum of the solid curves. A quasi-particle which occupies a sloping orbital exerts a driving force in γ. Occupation of both orbitals gives the $h_{11/2}$ S-band.

recently R. Bengtsson, et al.[16]

In discrete-line spectroscopy the two signatures are easily recognized provided that j is known. The sequence of spin states ....,j-2,j,j+2,... belongs to the favored signature and the sequence ...,j-1,j+1,j+3,... belongs to the unfavored signature. The signature splitting appears as an energy staggering between alternating spins, and is easy to extract by plotting the routhian versus rotational frequency ω.[11] Thus the set of diagrams presented in Fig. 4 should be a powerful tool for obtaining a first qualitative analysis of discrete-line spectra. The remainder of this section illustrates this point by a discussion of some current examples.

Positive γ-deformation has recently been deduced from the observed signature splitting at high spins in some $N \lesssim 90$ nuclei[16-19], and as a first example the main arguments will be reviewed on the basis of Fig. 4. The superfluid core is expected to have irrotational-like moments of inertia and thus be driven by rotation towards $\gamma = -30°$. The first band crossing comes from the rotational alignment of two $i_{13/2}$ neutrons, which corresponds to placing quasi-particles in the two orbitals of square 2 in Fig. 4. These quasi-particles drive the nucleus away from negative γ-values into the positive-γ sector. The effect on the signature splitting for an odd $h_{11/2}$ proton can be seen in square 3 which corresponds to the appropriate position of the Fermi level. There the $h_{11/2}$ signature splitting can be reduced or even inverted by going from γ at 0° or just below to positive γ. This change in the signature splitting is observed experimentally above the backbend.

A second example is the decrease in rotational alignment with increasing spin that has been noted in the

unfavored $i_{13/2}$ band of the nucleus ^{167}Yb.[20] Square 3 suggests a possible mechanism for this anomaly. If the core goes from 0° to negative γ with increasing spin, the unfavored rotational quasi-particle energy increases according to the diagram, which reflects primarily a loss of rotational alignment.

A third interesting region of rare-earth nuclei is the very lightest one, around ^{128}Ce, where both the proton and neutron Fermi levels are located inside the $h_{11/2}$ shell. A proton backbend would favor $\gamma = 0°$ (square 2 or 3), or equivalently be favored by 0°. A neutron backbend would favor or be favored by $\gamma = -40°$ (square 5). Whichever backbend is yrast depends on the rest of the nucleus. The potential energy is believed to slightly favor the protons, whereas the pairing gap is calculated to be smaller for neutrons and thus favors a neutron backbend[21,22]. Figure 5 shows results from a calculation of the total energy of the nucleus in the rotating frame, plotted versus γ at two frequencies ω. A minimization has been carried out with respect to ε-deformation, while the pairing gap parameters Δ_p and Δ_n are held fixed at 0.15 and 0.12 $\hbar\omega_o$, respectively. For ^{128}Ce, the calculation gives a γ-soft potential in the 0° to -60° collective sector at the lower ω. A stabilization can be seen at the higher ω around -40° and 0° due to neutron alignment and the onset of proton alignment, respectively. The effect of $h_{11/2}$ quasi-particles on the other nuclei in Fig. 5 can be understood on the basis of Fig. 4. An odd $h_{11/2}$ proton blocks out the proton backbend, but it also delays the neutron backbend since it exerts a driving force away from -40°. An experiment which might verify the predicted effect of neutron alignment on γ would be to look for a backbend in the odd-proton case.

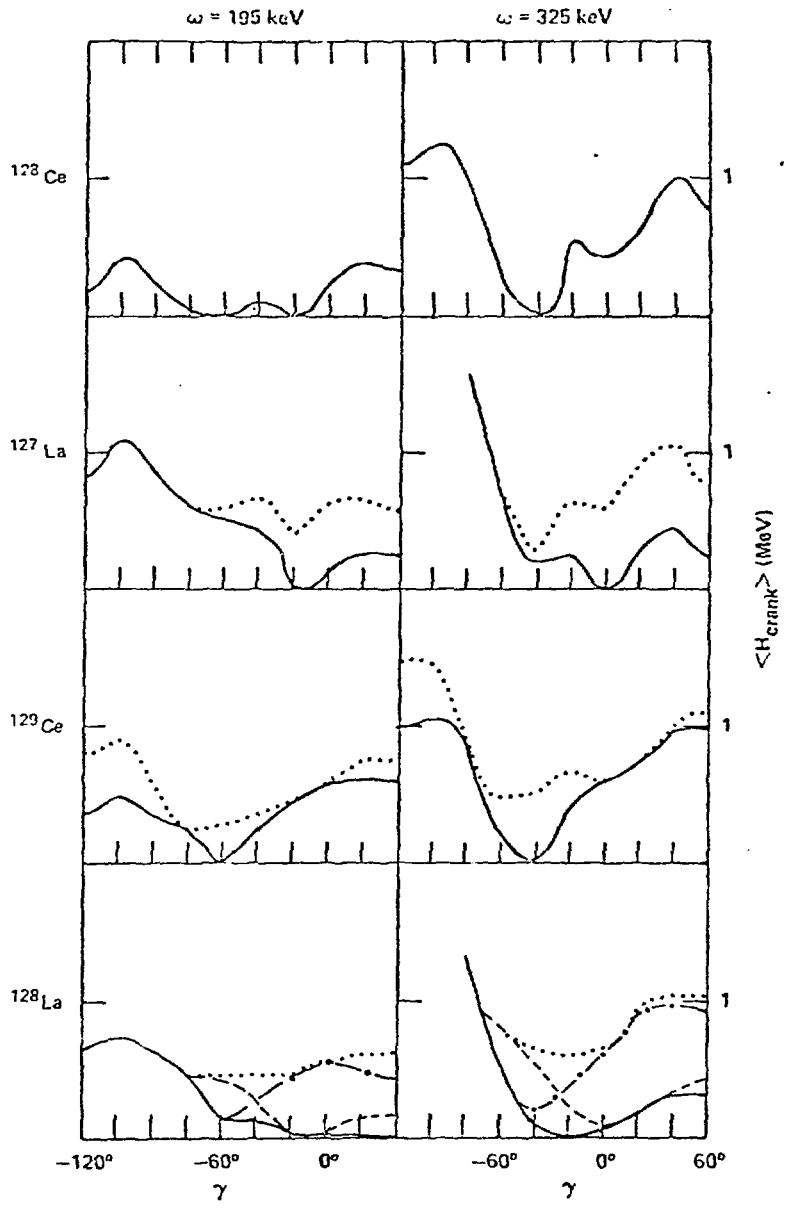

FIGURE 5. Similar to Fig. 4, but adiabatic routhians calculated at two frequencies for the entire nucleus ^{128}Ce and its neighbors, not just individual quasiparticle states. Both signatures are shown for the odd-A cases and all four combinations for the odd-odd case.

A neutron backbend taking the nucleus to -40° would cause a reduction of the proton $h_{11/2}$ signature splitting. Note the analogy with the $N \lesssim 90$ case described above, though here the mechanism is a large negative instead of a positive γ.

A numerical cranking calculation for some specific case, such as in Fig. 5, incorporates the high-j quasi-particle effects which can be read out of Fig. 4. An alternative approach which does not require extensive computing is suggested in Ref. 19 and is applied there to the $N \lesssim 90$ region. The idea is to take quasi-particle routhians from diagrams like Fig. 4 and to superimpose them on a phenomenological polarizable core. To the extent that the quasi-particle routhians are accurately described by the cranking model, a fit to experimental data can then be viewed as a phenomenological determination of basic core properties, for example, the prolate-oblate difference in the adiabatic potential-energy surface.

In summary, it is suggested that a large body of spectroscopic data might be interpreted using Fig. 4. The basic feature is the smooth variation of the γ-polarization with λ. The same general picture should be applicable in all regions of γ-soft nuclei throughout the chart of nuclides. It would be interesting to test experimentally whether all the different ranges of γ do in fact occur. The experimental evidence can come from signature splitting, as discussed above, and from the B(E2) values which are proportional to $\cos^2(\gamma + 30°)$. In particular, it would be valuable to identify large negative γ-values at high spins. These might occur in rare-earth nuclei with neutron number somewhat below 80 and also in the Hg-Pt region (Fig. 9 below).

Finally, it may be mentioned that the γ-polarization

effect of a high-j shell is qualitatively similar when the calculation is done without pairing. With this information about the role played by high-j shells in determining γ, we proceed to the second step of the analysis.

III. THE HARMONIC OSCILLATOR 'CORE'

The cranked harmonic oscillator is a model which does not have high-j intruder shells and in that sense is similar to the nuclear 'core' alluded to in the previous section. The literature contains both exact numerical solutions[23] and a variety of analytical expressions valid at given deformation or for a valence space truncated to a single non-rotating major shell[10]. The following treatment applies to such configurations in a single N-shell, using the approximations of Cerkaski and Szymański[24] but with a minor modification[25] that makes the rotational bands perfectly parabolic as a function of spin I. The purpose here is to survey the entire set of configurations that can be constructed in an N-shell that is somewhat larger than the ones considered in most of the recent literature on the cranked harmonic oscillator. Specifically, it is the N=4 shell which is considered below for three different cases: half full, nearly empty, and nearly full. The number of particles in the N=4 shell is 2×14, 2×4, and 2×26, respectively, taking into account protons and neutrons and also spin degeneracy. In order to keep the number of configurations down, the proton and neutron configurations are taken to be identical under the assumption that additional configurations would only generate a vast number of states with properties intermediate between those of the states included here.

The properties of a rotational band follow[24] from three

quantum numbers, Σ_1, Σ_2, and Σ_3, which can be evaluated for the non-rotating band head as

$$\Sigma_i = \sum_{\text{occ.}} (n_i + 1/2)$$

where the sum runs over all the occupied single-particle states and n_i is the number of oscillator quanta along the i-axis. By convention, $\Sigma_3 > \Sigma_2 > \Sigma_1$.

Some properties of the lowest band heads are plotted in Fig. 6. There the energy is obtained as

$$E_o = \Sigma_1 \overset{\circ}{\omega}_1 + \Sigma_2 \overset{\circ}{\omega}_2 + \Sigma_3 \overset{\circ}{\omega}_3$$

with

$$\overset{\circ}{\omega}_i = (\Sigma_1\Sigma_2\Sigma_3)^{1/3}/\Sigma_i$$

and the γ-deformation of the band head is given by

$$|\gamma| = \arctan \frac{\sqrt{3}}{2} \frac{\frac{1}{\Sigma_1} - \frac{1}{\Sigma_2}}{\frac{1}{2}\left(\frac{1}{\Sigma_1} + \frac{1}{\Sigma_2}\right) - \frac{1}{\Sigma_3}} \qquad (0° < |\gamma| < 60°)$$

It is given as an absolute value since the axis of rotation has not yet been specified. Figure 6 shows that the ground state is near prolate at the bottom of the shell and near oblate at the top of the shell. At midshell the two lowest configurations are the ones which minimize Σ_1 and maximize Σ_3, leading to near oblate and near prolate triaxial shapes, respectively. Disregarding the ground states, the main impression conveyed by Fig. 6 is that the excited configurations distribute themselves rather evenly over all values of γ. A quasicontinuum spectrum would show average properties of the corresponding rotational bands.

The system can be cranked around one of the three

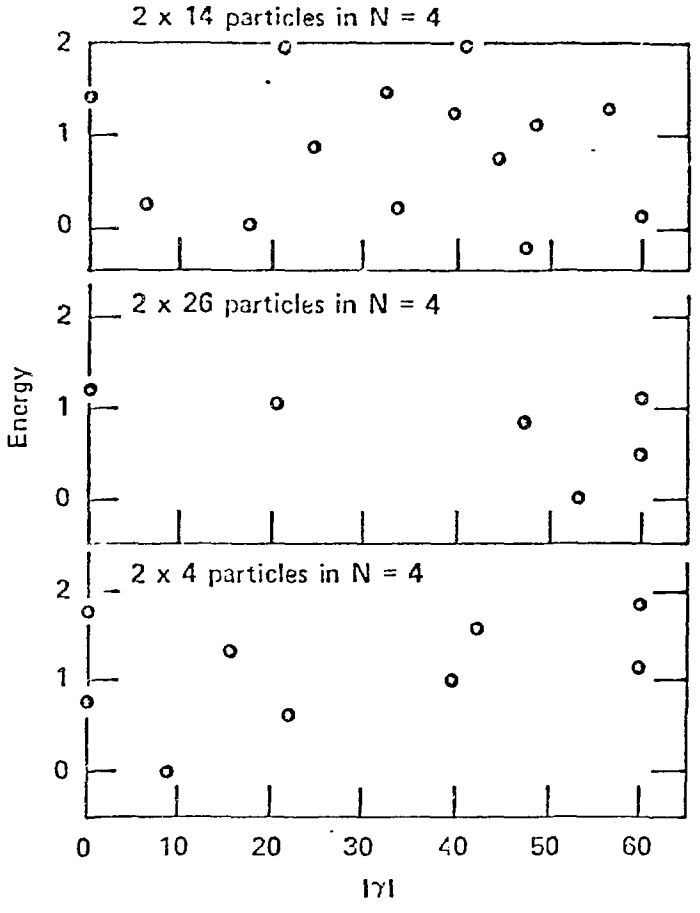

FIGURE 6. The energy in oscillator units and the γ deformation of low-lying states in a non-rotating harmonic oscillator potential. It is filled to the middle of the N=4 shell, almost to the top and just above the bottom of that shell, respectively. Zero energy is defined by the state with maximum number of oscillator quanta along one axis. The excited states are seen to spread fairly evenly over γ.

principal axes, and in a technical sense, this generates three rotational bands on each band head. The moments of inertia are

$$\mathcal{J}_i = 2\left(\Sigma_1\Sigma_2\Sigma_3\right)^{2/3}/\Sigma_i .$$

This expression is derived from the in-band energies, but also coincides with the rigid-body moment of inertia at the band-head deformation. The rotation corresponds to $\gamma > 0°$, $0° > \gamma > -60°$, and $-60° > \gamma > -120°$ for $i = 1,2,3$, respectively, near the band head. The evolution of γ in going to higher spins is shown schematically in Fig. 1. The lowest band is referred to by Cerkaski and Szymański[24] as the L-band. It is obtained by rotation around the 1-axis and lies in the sector $\gamma > 0°$. The L-band terminates at $\gamma = +60°$ and maximum spin I_{max}, where

$$I_{max} = \Sigma_3 - \Sigma_2.$$

The value of γ changes with increasing rapidity as I_{max} is approached from below within the band and reaches the aligned single-particle limit $+60°$ at I_{max}. Cranking around one of the other axes instead gives rise to the medium (M-) band or the highest (H-) band. These start in the other 60° sectors of γ and rise to their respective single-particle limits at a maximum spin equal to the difference between the perpendicular Σ-values. The H-band goes to $-120°$ and the M-band goes to $+60°$ except when the band head is nearly oblate. In that case, the M-band goes to $-120°$. It seems likely that these general trends might persist in the diabatic bands of a realistic model, even if the adiabatic potential-energy minimum behaves differently.

The M-band reaches higher spins than the other bands since $\Sigma_3 - \Sigma_1$ gives the largest I_{max}. The rotation around this intermediate axis is classically unstable, but taking into account additional half-filled high-j shells or simply high spins beyond the L-band cutoff, the M-band becomes lowest and therefore stable.

The moment of inertia $\mathcal{J}$ and the maximum spin I_{max} for

all the bands of a half-full N=4 shell are displayed in Fig. 7. Most striking is the small spread in the moment of inertia, although the different bands represent the full range of γ-values and subsequently both collective and single-particle modes of rotation. Since the bands are parabolic, this is true for both $\mathcal{J}^{(1)}$ and $\mathcal{J}^{(2)}$. The implication is that a single moment of inertia might emerge from many bands even in a γ-soft nucleus, and might thus be evidenced in quasicontinuum spectra.

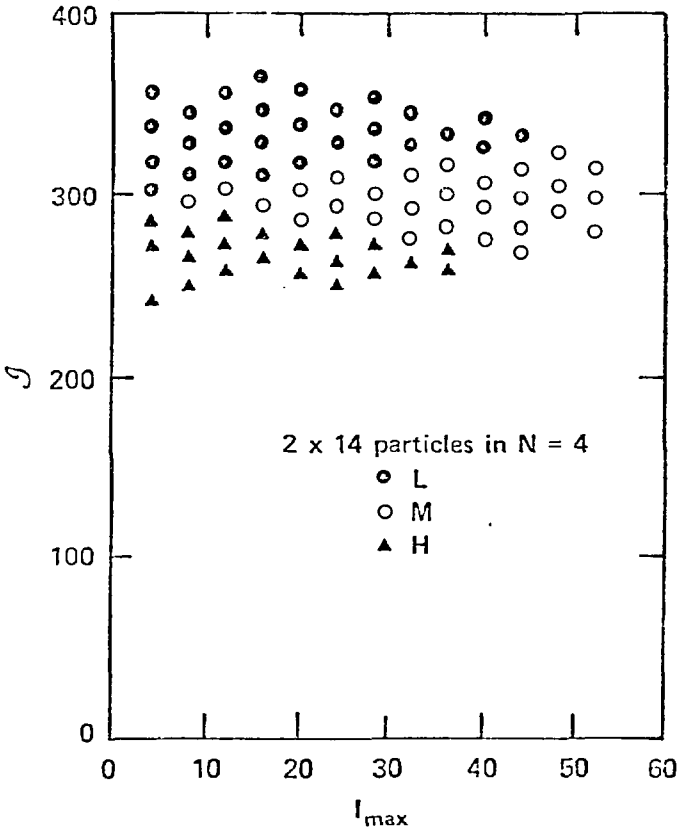

FIGURE 7. The moment of inertia in oscillator units and the maximum spin of cranked harmonic oscillator bands with the N=4 shell half filled. Note the small spread in $\mathcal{J}$.

A larger spread in the moment of inertia can be achieved by promoting particles to higher N-shells. This is expected to occur at high spins along the nuclear yrast line. The present analytical model is not suitable for exploring such an extension of the configuration space, however. By redistributing particles over the N-shells in the mid-shell case -- from 2 × (20,14,0,0) to 2 × (14,12,6,2) particles for (N<4,N=4,N=5,N=6) -- we find a super-deformed band head $(\Sigma_1,\Sigma_2,\Sigma_3)$ = (106,122,254) at lower energy than the ground state.

Figure 8 is similar to Fig. 7, but for the almost empty and almost full N=4 shells. A feature of interest in the latter case is the low maximum spin that can be eked out of the L-bands. The in-shell yrast states at high spins thus belong to M-bands which are mostly negative in γ. Coherence between the harmonic oscillator 'core' and the high-j shells can therefore be expected in almost full major shells, favoring negative γ.

IV. SOME CALCULATIONS FOR NUCLEI AT VERY HIGH SPINS

The cranked modified oscillator[8,12] is a model where the j-shells are displaced by additional $\underset{\sim}{l}\cdot\underset{\sim}{s}$ and $\underset{\sim}{l}^2$ terms in the potential. Predictions of yrast shape regimes at very high spin from this model have been confirmed on the whole by experiments so far, most recently in data presented by Baktash[26] at this conference. Figure 9 shows the regimes of γ deformation obtained as yrast in calculations by the Lund group over a wide range of nuclei[9]. These calculations are formally made for spin I = 20, but without pairing which means that the results are more likely to be relevant at higher spins where both proton and neutron rotation-aligned quasi-particles contribute to the spin of

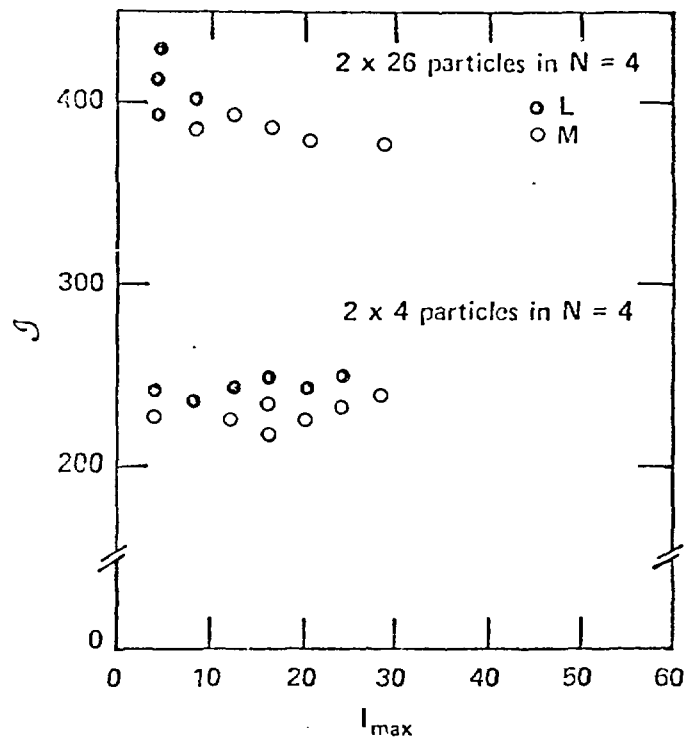

FIGURE 8. Same as Fig. 7, but for a nearly full and nearly empty N=4 shell. Only the M-bands reach up to high spins for the nearly full shell.

the nucleus. Each regime of γ is seen to occur as yrast in certain nuclei. The notation relates to the (ε,γ) plane of Fig. 1 according to the insert in the lower right corner of Fig. 9. For example, collective bands with large negative γ ('c' and 'd') can be found just below shell closures, for reasons explained above. However, when theoretical results are presented in this way, it is important to keep in mind that a statement is being made only about one of the configurations expected to lie at or near the yrast line. For the large number of cases where the potential energy is soft or has several minima[9], other low-lying configurations

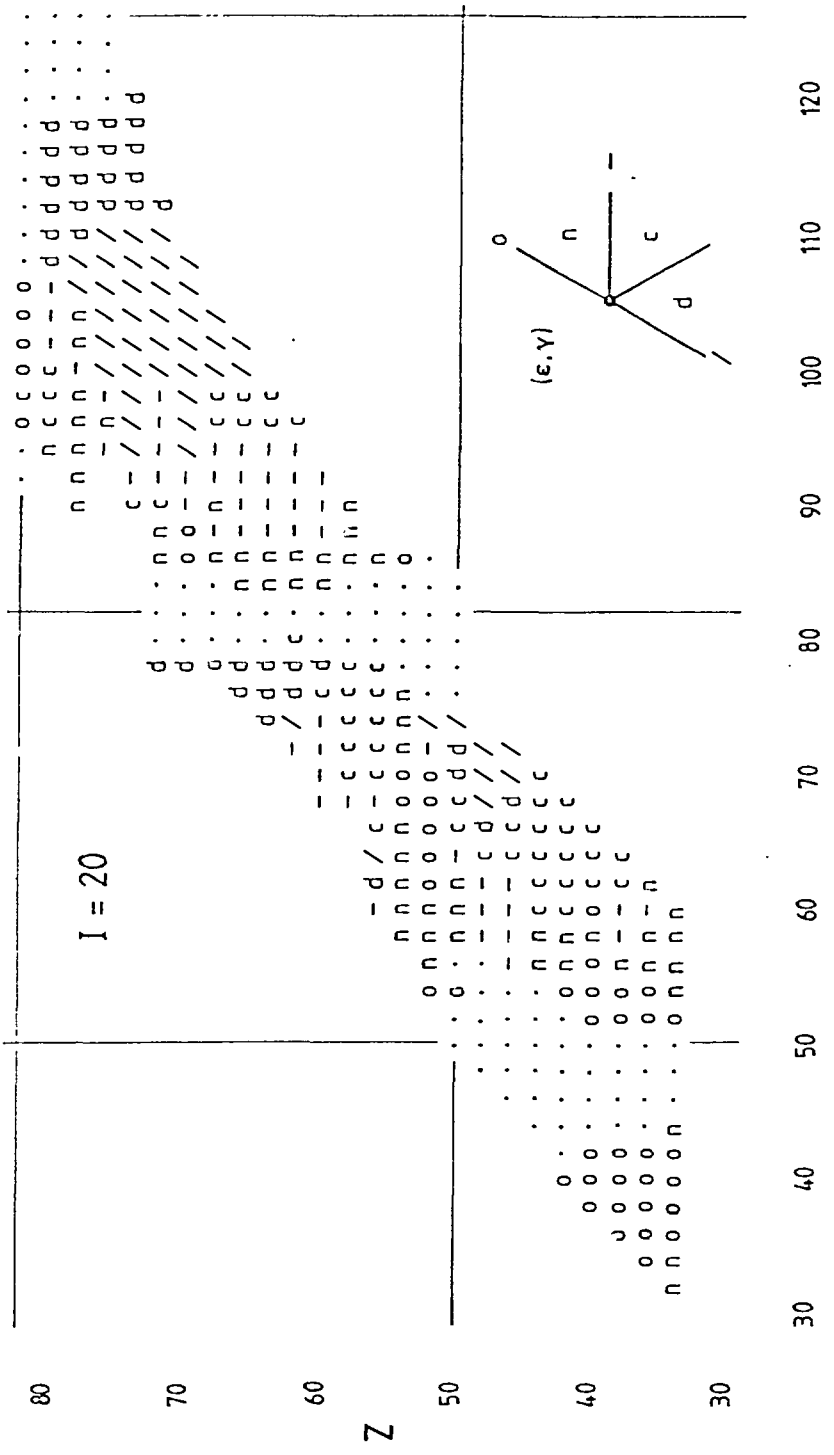

FIGURE 9

have quite different properties. Such coexistence of shapes in experimental discrete line spectra has been emphasized for many years by Hamilton[27] and clearly occurs, for example, in the N~87 spectra presented at this conference[26,28].

An interesting calculation was recently made for very high spins in ^{158}Er by T. Bengtsson and Ragnarsson[29], who have devised a method to construct the diabatic states of both yrast and non-yrast bands from the cranking model solutions. The previous picture, from the calculated potential-energy surfaces[9], is that ^{158}Er becomes soft at high spins in the 0° to +60° sector of γ and a transition between the prolate collective and oblate single-particle regimes occurs between I = 40 and 50. The picture obtained[29] by actually constructing sequences of states belonging to specific configurations is reproduced in Fig. 10. There, bands are seen to occur at a variety of deformations, though all moving towards γ = +60° with increasing spin like the L-bands of the harmonic oscillator. The bands in Fig. 10 are all intertwined along the yrast line.

The implication for quasicontinuum spectroscopy is that the bumps in an energy spectrum may have several structural origins. For example, M1 gamma rays of 600-700 keV in ^{158}Er may arise from:

i) Cascades along bands starting at oblate and going into the γ-plane, for those cases where such bands are signature degenerate[29]. The competing collective E2 transitions are weak as long as γ is large and positive.

ii) 'Statistical' transitions between oblate states. However, oblateness is to some extent not a regime in this nucleus but a property common to the uppermost member of each band.

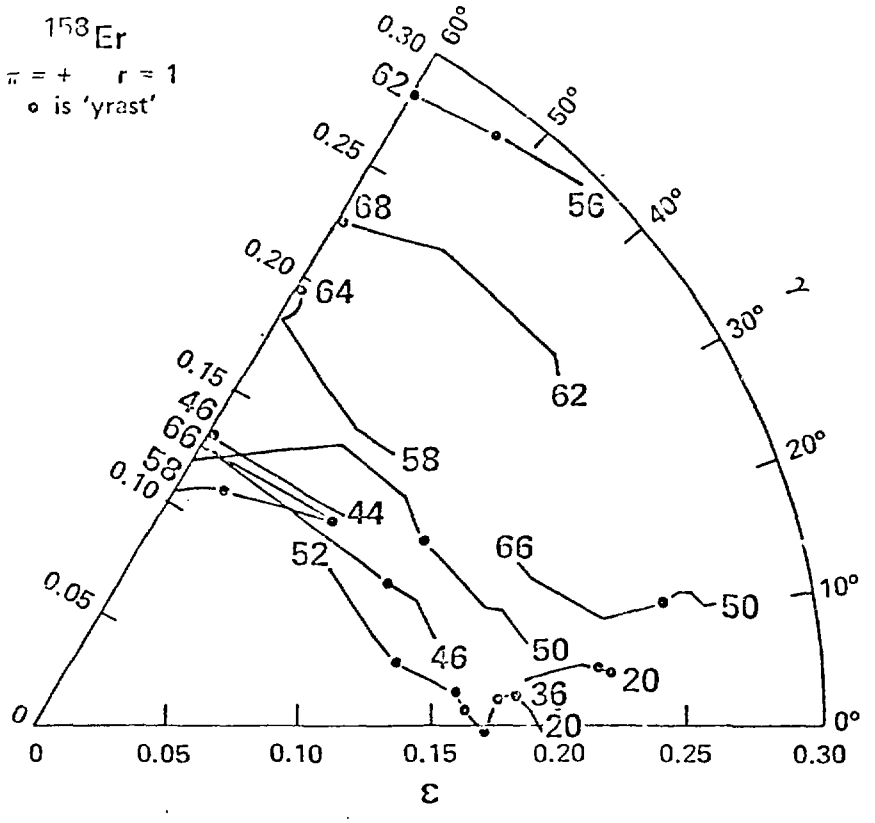

FIGURE 10. The changing (ε,γ) deformation along segments of rotational bands, between the spins indicated at the ends. The bands have been calculated for ^{158}Er with the cranked modified oscillator by T. Bengtsson and Ragnarsson[29]. The large dots represent states which are yrast relative to other states with $\pi = +$ and $r \equiv e^{-i\pi\alpha} = +1$, and the bands shown are those which contain at least one such state.

iii) High-K bands, built on the most strongly deformed oblate states[30].

Quadrupole E2 gamma rays of about twice the M1 energy can arise from any of the bands. At $I > 50$ an especially strong source must be bands like the one near $\varepsilon = 0.25$, $\gamma = 10°$. This configuration is driven toward the collective

regime by a more-than-half-full proton $h_{11/2}$ shell (c.f. Section II above).

V. SUMMARY AND CONCLUSIONS

The γ shape degree of freedom has been studied in a rotating high-j shell, a harmonic oscillator, and a modified oscillator potential.

It was previously known that a rotating quasiparticle in a high-j shell may influence the γ-deformation due to the shape of its orbit and the resulting polarization of the core. Figure 2 above brings out the systematics of this effect. The most favorable γ, corresponding to the shape of the lowest quasiparticle orbit, varies smoothly throughout the range of γ from $+60°$ to $-120°$ as the Fermi level moves up through the shell. A straightforward corollary of this rule is demonstrated by Fig. 4: the signature splitting is large at the preferred γ, small or inverted at other γ-values. Measurements to detect changes of signature splitting would be valuable to test this simple picture of static shape polarization. In particular, there is no evidence yet for the existence of triaxial shapes with large negative γ at high spins.

The in-shell bands of the harmonic oscillator 'core' exhibit a large spread in γ but a small spread in the moment of inertia. This and other trends of the harmonic oscillator appear to persist alongside the effects due to high-j shells in the more realistic modified oscillator model. A consequence of the competing trends in γ-soft nuclei is the coexistence of several differently structured sequences of levels or bands following the yrast line.

UNISOR is a consortium of twelve institutions, supported by them and by the Office of Energy Research of the U.S.

Department of Energy under Contract No. DE-AC05-760R00033 with Oak Ridge Associated Universities.

One of us (G.L.) wishes to acknowledge valuable discussions with R. Bengtsson and I. Ragnarsson.

REFERENCES

1. K. Kumar and M. Baranger, Nucl. Phys. A110, 529 (1968).
2. D. A. Arseniev, A. Sobiczewski, and V. G. Soloviev, Nucl. Phys. A139, 269 (1969).
3. U. Götz, H. C. Pauli, K. Alder, and K. Junker, Nucl. Phys. A192, 1 (1972).
4. S. E. Larsson, Phys. Scr. 8, 17 (1973).
5. A. Faessler, J. E. Galonska, U. Götz, and H. C. Pauli, Nucl. Phys. A230, 302 (1974).
6. D. Ardouin, R. Tamisier, M. Vergnes, G. Rotband, J. Kalifa, G. Berrier, and B. Grammaticos, Phys. Rev. C 12, 1754 (1975).
7. S. E. Larsson, G. Leander, I. Ragnarsson, and N. G. Alenius, Nucl. Phys. A261, 77 (1976).
8. G. Andersson, S. E. Larsson, G. Leander, P. Möller, S. G. Nilsson, I. Ragnarsson, S. Åberg, R. Bengtsson, J. Dudek, B. Nerlo-Pomorska, K. Pomorski, and Z. Z. Szymański, Nucl. Phys. A268, 205 (1976).
9. S. Åberg, Phys. Scr. 25, 113 (1982).
10. A. Bohr and B. R. Mottelson, Nuclear Structure, Vol. 2 (Benjamin, New York, 1975).
11. R. Bengtsson and S. Frauendorf, Nucl. Phys. A327, 139 (1979).
12. K. Neergaard, V. V. Pashkevich, and S. Frauendorf, Nucl. Phys. A262, 61 (1976).
13. S. Frauendorf, Nucl. Phys.; Proc. Nuclear Physics Workshop, ICPT Trieste, 1981, ed. by C. H. Dasso, p. 111.
14. F. S. Stephens, Rev. Mod. Phys. 47, 43 (1975).
15. J. Meyer-ter-Vehn, Nucl. Phys. A249, 111 and 141 (1975).
16. R. Bengtsson, F. R. May, and J. A. Pinston, Proc. XX Int. Winter Meeting on Nuclear Physics, Bormio, 1982, p. 144.
17. R. Bengtsson, J. A. Pinston, D. Barneaud, E. Monnand, and F. Schussler, Nucl. Phys. A, in press.
18. L. L. Riedinger, Phys. Scr., in press.
19. S. Frauendorf and F. R. May, sub. to Phys. Lett. B.

20. J. Almberger, I. Hamamoto, and G. Leander, Nucl. Phys. A333, 184 (1980).
21. P. Möller and J. R. Nix, At. Data & Nucl. Data Tables 26, 165 (1981).
22. G. A. Leander, P. Arve, T. Bengtsson, I. Ragnarsson, and J. Y. Zhang, Nucl. Phys. A, in press.
23. T. Troudet and R. Arvieu, Ann. of Phys. (N.Y.) 133, (1981).
24. M. Cerkaski and Z. Szymański, Acta Phys. Pol. B10, 163 (1979).
25. H. Sagawa and T. Dössing, Phys. Lett. 96B, 238 (1980).
26. C. Baktash, these proceedings.
27. J. H. Hamilton, Proc. Int. Conf. on Selected Topics in Nuclear Structure, ed. by V. G. Soloviev, et al. (Dubna, USSR, 1976), Vol. 2, p. 303; and Proc. Int. Symp. on Nuclear Collectivity, Dogashima, Japan, 1982.
28. R. Kroth, P. Aguer, G. Bastin, H. Hübel, L. Nguyen, H. Sergolle, and J. P. Thibaud, Contr. to this conference, p. 90.
29. T. Bengtsson and I. Ragnarsson, Phys. Scr., in press.
30. P. Arve, Y. S. Chen, and G. A. Leander, Phys. Scr., in press.